Potential Field Source Surface Models: A Comparative Study

B.Bala and X. P. Zhao

Hansen Experimental Physics Laboratory, Stanford University, Palo Alto, CA 94304

Abstract

The main objective of Space Weather is the prediction of solar wind properties at 1 AU. It has been established that there exists an inverse correlation between the flux expansion factor (FTE), obtained using a potential field source surface model (PFSS), and the solar wind speed at 1 AU. This inverse correlation has been made use of in the prediction of solar wind speed and interplanetary magnetic field at 1 AU with reasonable accuracy. However, PFSS models do not take the effects of all the currents in the corona into account, leading to an underestimation of the total flux escaping into the heliosphere. Also, there have been discrepancies in the predicted and observed solar wind speed, especially at high latitudes. Recently, several models that include various currents in the calculation of coronal magnetic field have been put forth. The present work is a comparison of one such model, the Current Sheet–Source Surface model (CSSS), with the PFSS model and the observed solar wind speed at 1 AU. This is aimed at obtaining a relation, between the flux expansion factor and the solar wind speed, that predicts both the ecliptic and high latitude solar wind with sufficient accuracy.

Potential Field Source Surface (SS) Model

Assumptions

- Coronal field is a potential field
- Field at source surface, at 2.5 $R_\odot$, is purely radial

Corrections to the data

- Eliminated the zero offset
- Added a strong polar field
- Reconstructed missing data

Free parameters:

- Height of the source surface 2.5 or 2.35 $R_\odot$: we used 2.5 $R_\odot$
- The radius of the inner surface: 1.0 $R_\odot$

Current Sheet–Source Surface (CSSS) Model

Improvements over SS model

- Source surface is placed near the Alfvén critical point where all the magnetic fields are radial
- Introduced a cusp surface, where field lines are open but not necessarily radial, to include effects of streamer current sheets
- Used the source surface technique to include the effects of volume currents beyond the source surface

Free parameters

- a = 0.2 ; the height distribution of the horizontal current
- $R_{cp} = 2.0$; heliocentric distance of the cusp surface
- $R_{ss} = 15.0$; heliocentric distance of the source surface

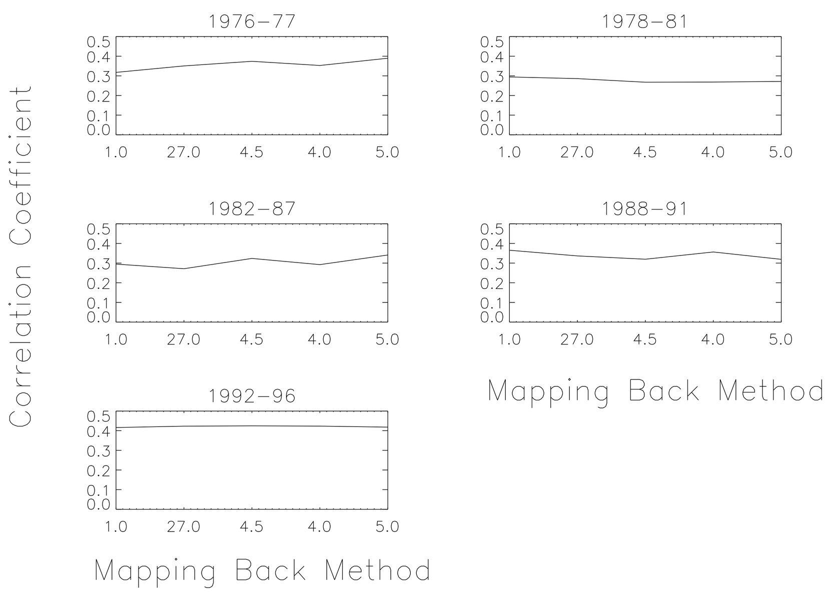

Figure 1a. Correlation coefficient for different mapping back method and different phases of solar cycle for SS model.

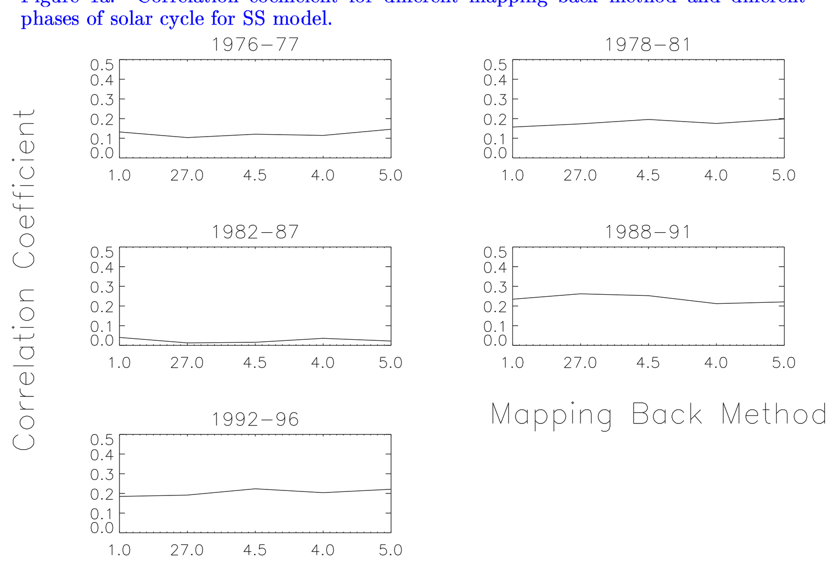

Figure 1b. Same as Figure 1a but for CSSS model

Data and Procedure

- Photospheric magnetic field data: daily updated Wilcox Solar Observatory synoptic data as well as Kitt Peak data.
- Latitude for calculating FTE: b0 angle corresponding to the observed solar wind location
- Longitude: inverse mapping of solar wind at 1 AU assuming radial flow along the Archemedian spiral. Different authors have taken different transit times at different occassions for inverse mapping. Therefore, to see the sensitivity of the correlation between FTE and SWS to the inverse mapping technique, we used all possible transit times:
  1. 4 days, 4.5 days or 5 days (Neugebauer et al., , 2002)
  2. 27-day running average of the observed solar wind speed (Wang et al., 1997)
  3. observed daily solar wind speed (SWS)

Flux Expansion Factor *vs* Solar Wind Speed

FTE has been calculated for each point on the source surface corresponding to daily solar wind using SS and CSSS models.

In this case, we used $N_{max} = 22$. Justification: (a) Zhao has shown that $N_{max} = 22$ has the closest reproduction of photospheric field using SS model. (b) Figure 4, where there is little fluctuation above $N_{max} = 22$

Figure 1: Variation of correlation coefficient, for SS and CSSS models, with phase of solar cycle and for different inverse mapping, mentioned earlier. Note that the correlation does change with both the phase of the solar cycle and inverse mapping. However, the changes are not highly significant.

Figure 2: Scatter plot of FTE *vs* SWS, for SS model, for the declining phase 1992–96. The correlation coefficient is given in the figure. "map back 1.0" implies inverse mapping method 3.

As Wang and Sheeley have already established, there is an inverse correlation between FTE on source surface and SWS at 1 AU. The correlation is lower in the case of CSSS model which may be because the free parameters are not selected appropriately. However, it is to emphasized that there is large scatter about this mean trend, as mentioned by Wang and Sheeley (1995). The physical significance of this scatter is explored and the results are presented in the following section.

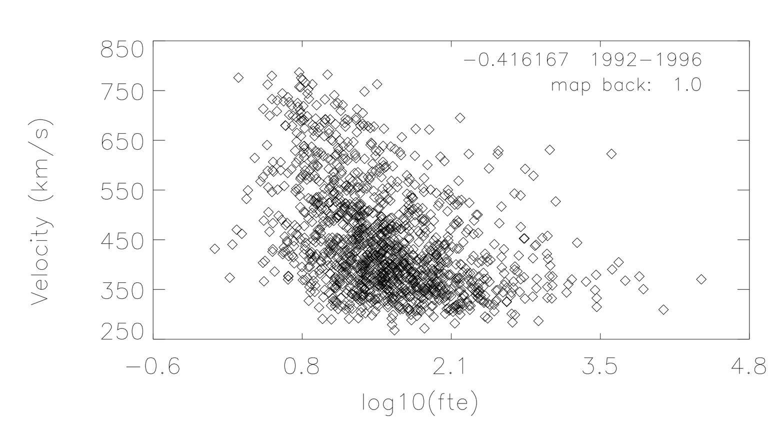

Figure 2. Scatter plot of FTE *vs* SWS for SS model

"Scatter" in the Scatter Plot

Figure 3(a) **Top:** Daily averaged solar wind speed taken from the OMNI data (triangles). Solid circles represent slow solar wind (≤ 450) km s^{-1} corresponding to which FTE is less than 20, a discrepancy causing the "scatter" in Figure 2. **Bottom:** The latitude and longitude of this discrepancy.

Figure 3(b) The solar wind v-map for CR 1894–1896 using the IPS data corrected using tomography.

Figure 3(c) The HeI 1083nm coronal hole map from Kitt Peak for CR1894.

These figures suggest interaction of fast and slow streams. This aspect will be addressed in detail in a future work.

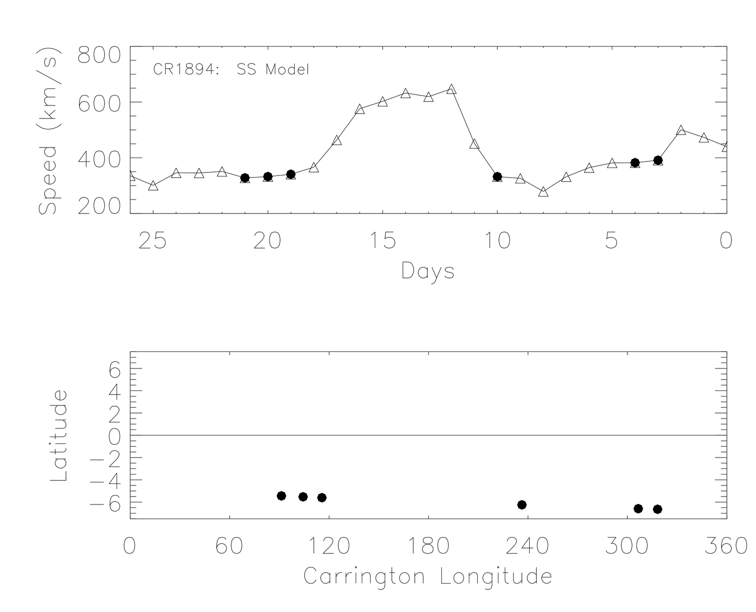

Figure 3a. Top: Daily solar wind speed. Bottom: The latitude and longitude corresponding to the circles in top panel.

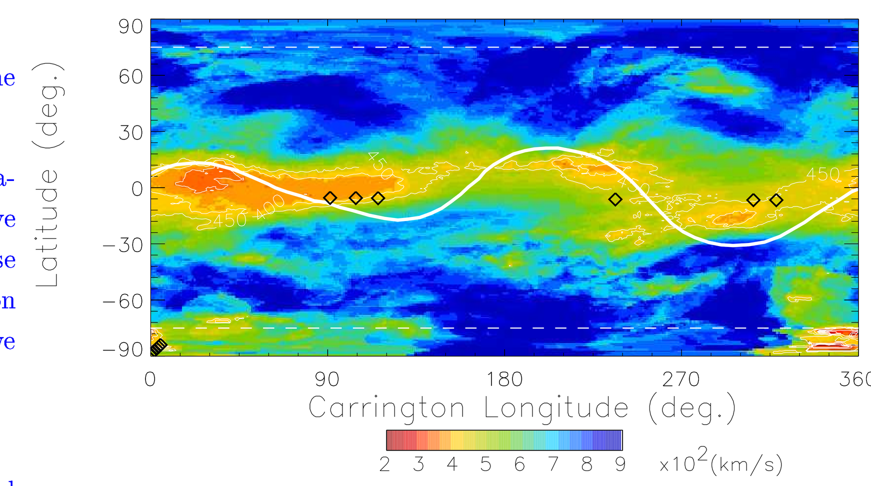

Figure 3b. IPS v-map after applying tomography for CR1894. The thick solid line is the neutral line derived from SS model calculation. The diamonds represent the location marked by solid circles in Figure 3a.

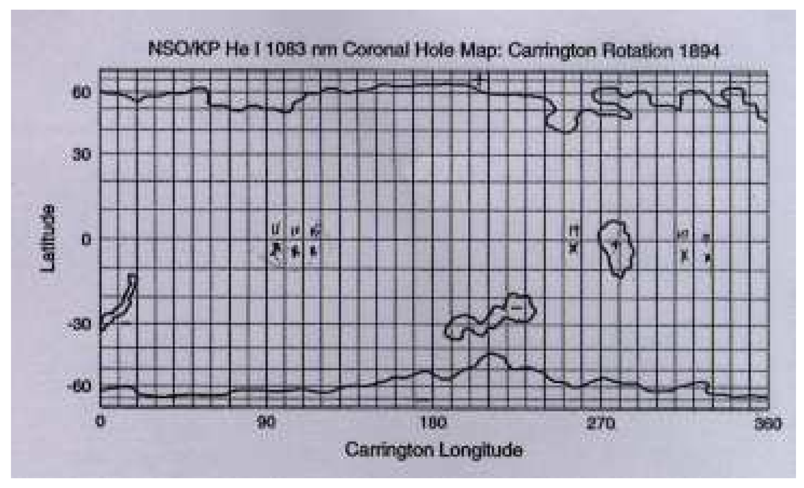

Figure 3c. He I 1083 nm Coronal hole synoptic map from Kitt Peak for CR1894.

Variation of θ and ϕ with N_{max}

Figure 4a and 4b show Variation of θ and ϕ respectively, with N_{max} for CR 1829 (1990), computed using SS model and WSO data and plotted as a deviation from $N_{max} = 9$. Horizontal dashed line correspond to $N_{max} = 22$ and vertical dashed line, $\delta\theta$, $\delta\phi = 0$. A number of source surface locations were studied and the values were found to be fluctuating between ± 2, on average. Fluctuations larger than this are shown in Figure 4. The fluctuation depends on location on source surface (θ_{ss}, ϕ_{ss}) though not in a systematic way. The highest deviation in the case of θ, is for location (15, 170), about 15°. In most cases, there is little difference above $N_{max} = 22$ and the difference is largest between $N_{max} = 9$ and $N_{max} = 10$, 11 or 12. Fluctuations in ϕ are much larger than this, with the highest for the same location (15, 170), about 60°.

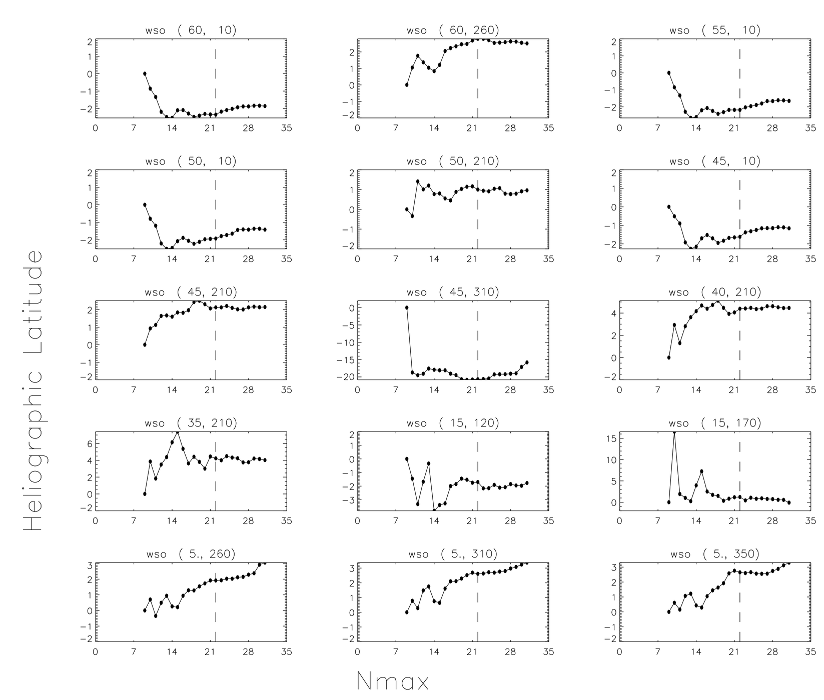

Figure 4a. Variation of θ with N_{max}, using SS model. The vertical line corresponds to $N_{max} = 22$.

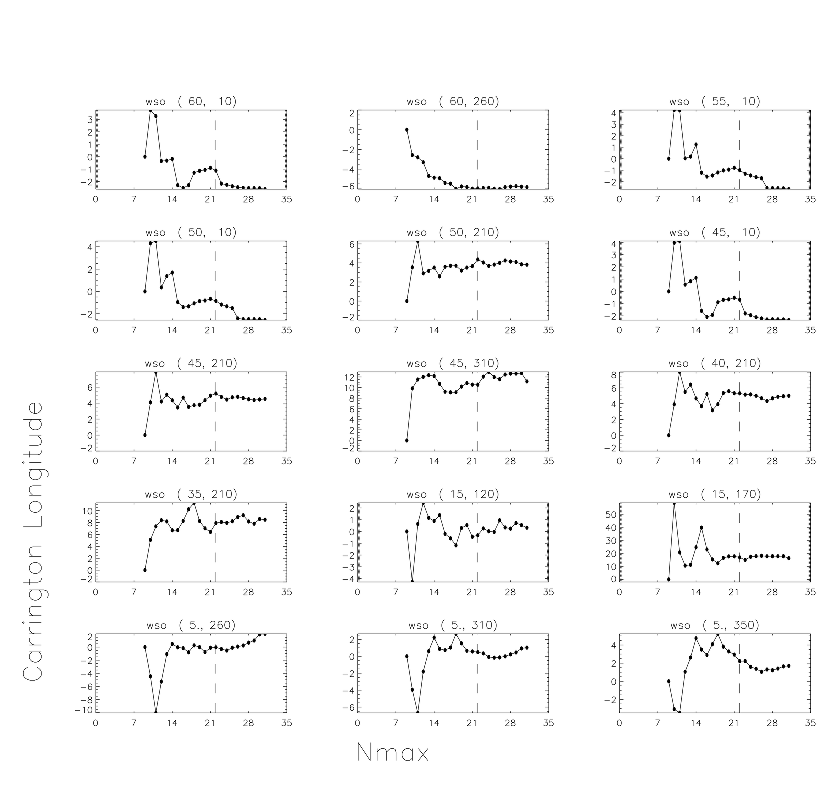

Figure 4b. Same as Figure 4a but for ϕ.

Variation of FTE with N_{max}

Figures 5a, 5b: Variation of FTE with N_{max} using SS and CSSS models respectively. Note that FTE is highly fluctuating with N_{max}. According to Wang and Sheeley (1990; 1994; 1997) FTE > 20 correspond to solar wind speed ≤ 450 km s^{-1}. For FTE in this range, e.g., location (45,310), where FTE varies between 40 and 55, it affects the solar wind speed in its finer details. In all other cases the fluctuation is over the entire range of FTE given by Wang and Sheeley. Such a variation implies that depending on the N_{max} used in the model, the solar wind emanating from a given point (θ_{ss}, ϕ_{ss}) on the source surface can be anywhere between 300 and 900 km s^{-1}!! This in turn implies that the prediction of solar wind speed based on PFSS model becomes "unpredictable", or highly dependent on one of the free parameters in the model.

Discussion and Concluding Remarks

Calculation of FTE depends on N_{max} and inverse mapping. A "wrong" selection of inverse mapping technique can lead to considerable discrepancies. From Figure 1, the observed daily values of solar wind seems a reasonable method. N_{max} changes FTE significantly leading to wrong prediction of solar wind at 1 AU. However, the best choice of N_{max} is still not clear though $N_{max} = 22$ could be reasonable. Next, the change of correlation coefficient with phase of solar cycle: periods 1982–1987 and 1992–1996 are declining phases but correlation coefficient differs by a factor of 1.5. This remains to be explained. Ulysses observations show that high speed wind remains rather constant at all latitudes. Figures 2 and 3 give the impression that not all solar wind come from open field regions. If slow solar wind is not emanating from boundaries of coronal holes, then where does it originate from? Most important, the relation:

$$f_s = \left(\frac{R_\odot}{R_{ss}}\right)^2 \frac{B_{R_\odot}}{B_{ss}}$$

implies that FTE is totally dependent on B_{ss} since there is little variation in the magnetic field $B_{R_\odot}$ inside coronal holes according to photospheric observation. SS model calculations show a large variation of B_{ss} from center to edge of coronal holes, but, Ulysses observations show that the interplanetary magnetic field is latitude independent. So, there is a discrepancy in the SS model calculation. Addressing these issues with the hope of finding satisfactory explanation will be our future task.

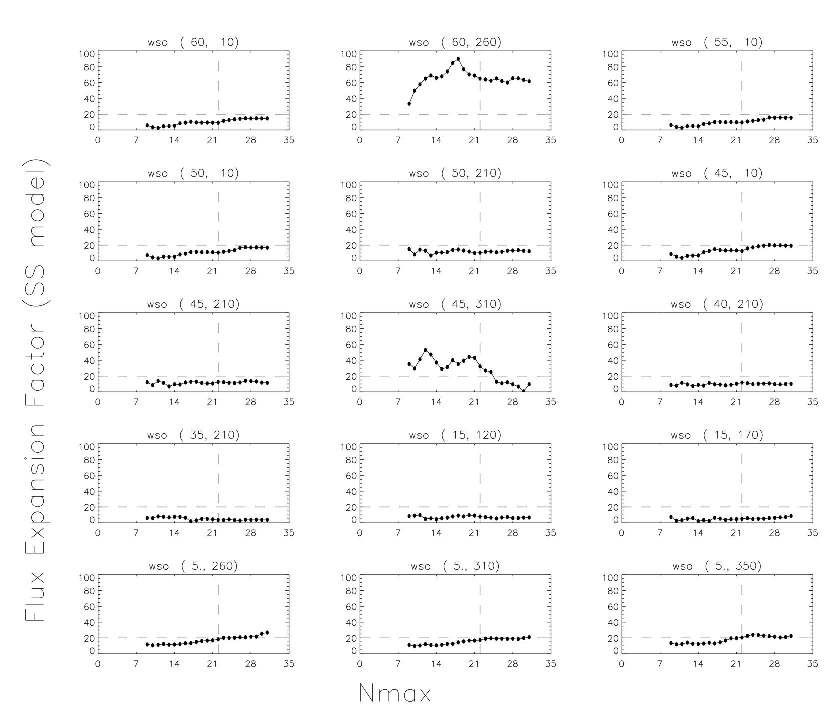

Figure 5a. Variation of FTE with N_{max}: SS model. The vertical line corresponds to $N_{max} = 22$.

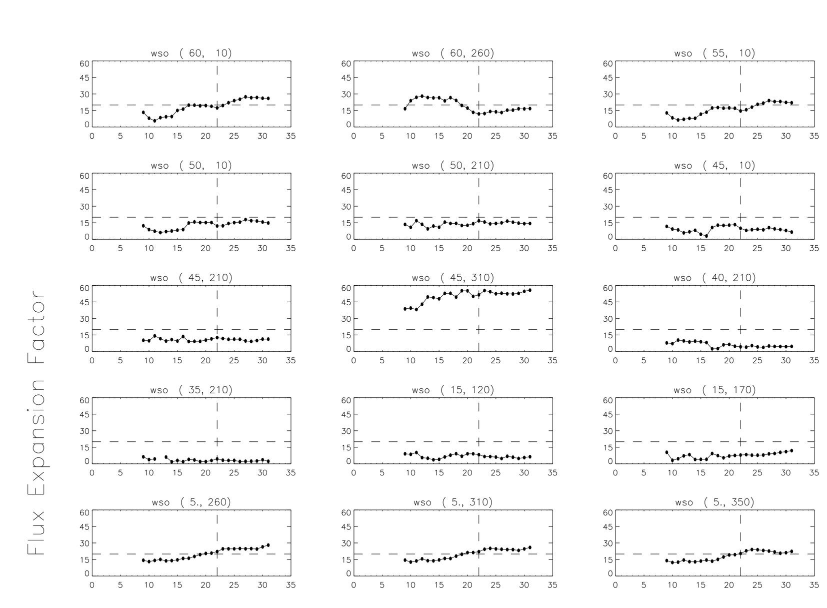

Figure 5b. Same as Figure 5a but for CSSS model.

References

Neugebauer et al., *Journal Geophys. Res.*, **107**, 2002

Wang et al., *Astrophys. J.*, **488**, L51–L54, 1997.

Wang, Y.-M., *Astrophys. J.*, **449**, L157-160, 1995.

Wang, Y.-M. and Sheeley, N. R., Jr., *Journal Geophys. Res.*, **99**, 6597–6608, 1994

Zhao, X.-P., and J. T. Hoeksema, *Journal Geophys. Res.* **100**, 19-33, 1995.